Paper

Design of steel cables against free-bending fatigue at terminations

Professor M. Raoof, BSc(Eng), MSc, PhD, DIC
School of Architecture & Civil Engineering, South Bank University

Synopsis
The present paper highlights the significant shortcomings of the traditional maximum (extreme fibre) stress (or strain) approaches for design against free-bending fatigue at the fixed ends to axially preloaded steel spiral strands in various fields of application.

The importance of catering for interwire/interlayer fretting in any realistic model for design against free-bending fatigue is emphasised. This is, then, followed by a brief review of the salient features of a promising theoretical model which takes interwire fretting into account. An extensive series of theoretical parametric studies, using a number of realistic spiral strand constructions covering a wide range of cable (and wire) diameters and lay angles, has been carried out in order to develop straightforward design formulations aimed at practising engineers.

The possible practical limitations of the final results are briefly discussed. Moreover, a numerical example is presented to facilitate use of the proposed alternative design procedure. The present formulations are amenable to simple hand calculations.

Notation

$A_i(t)$	is the amplitude of vibration in mode i as a function of time
A	is the wire cross-section area $= \pi r_w^2$
D_i	is the wire diameter in layer i (outer layer: $i = 1$)
d	is the strand outer diameter
E_δ	is Young's modulus for steel
$E_\delta,(EI)_{eff}$	is the strand overall bending stiffness
f	is the frequency
I	is the second moment of area
i	is the mode of vibration
K_{in}	is the no-slip interlayer shear stiffness
K_δ	$= \dfrac{T}{T_{ult.}}$
k	$= \dfrac{p}{2\pi}$
l	is the total cable span
m	is the cable mass/unit length
n_i	is the number of wires in layer i (outer layer: $i = 1$)
p	is the pitch of the helical wire in the outer layer $= \dfrac{2\pi r_1}{\tan\alpha_1}$
R	$= r_1 - r_w$
r_1	is the helix radius in the outer layer
r_w	is the wire radius in the outer layer
$\dot{S_1}$	is the strand mean axial strain
s	is the standard deviation to the fit
s'	is the estimated standard deviation of fitted σ_x
T	is the constant (mean) axial tension on the strand
$T_{ult.}$	is the ultimate tensile strength
U	is the interlayer slippage between wires in the vicinity of the so-called neutral axis (in plane-section bending terms)
u	is the displacement along the helical wire
$W(x',t)$	is the deflection function
x	is the trellis contact patch spacing between the outer and penultimate layers
x'	is the co-ordinate along the cable with origin at the support
x''	is the distance of an imposed concentrated load on a cable from the fixed end
y_b	is the bending amplitude (i.e. amplitude of conductor motion relative to clamp, measured a short distance from the clamp)
$y_{max.}$	is the free loop amplitude of vibration
α_1,α_2	are lay angles in the outer and penultimate layers, respectively
β	is the angle through which the cable is bent at the clamp by vibration
$\theta_o^{max.}$	is the polar angle at the fixed end where wire axial strain due to bending is maximum
θ_o	is the polar angle at the fixed end (always negative)
θ	is the polar angle anywhere along the cable
$\dot{\theta}$	is the nominal angular deflection at the socket $= \dfrac{y_b}{x''}$
μ	is the coefficient of interwire friction
ρ	is the radius of curvature at the fixed end
σ_x	is the tensile stress at the trailing edge of interlayer trellis contact patch
σ_x^f	is the fitted (mean) value of σ_x from the results in theoretical parametric study
σ_x^u	is the upper bound to σ_x
ψ	$= \alpha_1 - \alpha_2$
ω	$= 2\pi f$

Introduction

There is surprisingly little information available on fatigue performance of steel cables in free bending. The majority of published work concentrates on the influence of pulleys and sheaves as sources of wear and fatigue damage. This paper is concerned particularly with the bending effects in spiral strands in the absence of sheaves, fairleads, or other formers, so that the radius of curvature of strand is not predetermined.

Free-bending problems are a source of concern, and not infrequent failures, in structures ranging from suspension and cable-stayed bridge hangers and stays to guyed masts to electromechanical cables. Such fatigue failures invariably occur near partially restrained terminations of various types and wherever a rapid change in curvature is imposed.

In the case of cable-stayed bridges, for example, because of their flexibility, relatively small mass, very low structural damping and steadily increasing moving loads from heavier and higher-powered vehicles and trains, these structures are subjected to vibrational stress fluctuations and reversals: inspection of a large number of cable-stayed bridges around the world has revealed occurrence of cracks around the anchor joints of cables[1]. As discussed by Abdel-Gaffar & Khalifa[2], most vulnerable to vibrations due to wind, rain, and traffic, are the high strength cables which have very low damping ratios in the range 0.004 – 0.04[2,3]: under such conditions, the flexural stresses at the relatively rigid joints near the anchor heads can be of the same order of magnitude as the live-load-induced axial stresses, or sometimes even greater. There have been quite a few reported cases in which cables of cable-stayed bridges had to be replaced because of corrosion and fatigue problems[1]. In this context, it is also worth mentioning the well-publicised problems associated with the inclined hangers to the Severn Bridge.

For the free-bending of long cables under an approximately steady axial load, it is common to introduce a mathematically convenient, constant effective bending rigidity, $(EI)_{eff}$, for the cable, from which the radii of curvature at the points of restraint are calculated. The maximum bending strains in individual wires are then found on the basis of often semi-empirical formulations of a questionable nature: these strains are further assumed to govern the strand's bending fatigue life. Experimental and field observations, on the other hand, suggest the interwire fretting between counterlaid wires in various layers as the principal cause of wire fractures[4-6]. In fact, in a series of reversed free-bending fatigue tests on axially preloaded spiral strands, Hobbs & Ghavami[5] reported that the first wire breakages in the outer layer invariably occurred not at the extreme fibre (in plane-bending terms), but rather in wires very close to the neutral axis where the axial strain in the individual wires is very small.

The need for a reexamination of the traditional maximum stress approach to the free-bending fatigue problem is, therefore apparent and forms the basis of the present paper. In what follows, much attention will be devoted to developing a straightforward design method, aimed at practising engineers, which (as discussed later) takes the effect of interwire friction and fretting fully into account. This alternative, and still simple, approach is shown to largely overcome various shortcomings of the previously available maximum stress theories.

Previous work

Very little research has been performed on the fatigue behaviour of structural cables in free-bending near terminations. Hobbs & Smith[7] and Oplatka & Roth[8] are among the few researchers who transversely loaded steel cable specimens under constant tension to produce small amplitude free-bending near the socketed terminations.

The fatigue tests carried out by Hobbs & Smith[7] were on a series of 8.5m-long and 39 mm diameter spiral strands. Two levels of mean axial tension corresponding to 17 and 34 % of the maximum breaking load with bending amplitudes up to ±1.3° were imposed on the socketed steel strands whose ends were fixed against rotation. It was reported that wire breakages invariably occurred in the vicinity of the neutral axis (in plane-section bending terms) with the initial wire breakages starting in the outer layer and then proceeding to the second layer, finally leading to ultimate failure of the strand.

Oplatka & Roth[8] carried out a series of fatigue tests on 18 mm diameter six strand rope at a tension of 20 % of the maximum breaking load with bending amplitudes of ±4.5°. The socket was pinned and could rotate with the rope flexure while the bending motions were applied through the socket. Various forms of socket arrangements were tested in order to minimise the localised damage.

Tilly[8] reported free-bending fatigue data including 20 tests on five types of spiral strand and eight tests on two types of wire rope. These axially preloaded steel cable specimens had a free length between sockets of 2.8 m and were subjected to bending amplitudes up to ±2°. In particular, tests were stopped when five outer wire fractures were detected by visual inspection, although later examinations of dismantled cables identified the presence of some inner wire failures.

In the related field of overhead transmission lines, several measures of vibration intensity have been employed for developing fatigue curves through tests in laboratory spans, with limited success. The various parameters assumed to control free-bending fatigue life may be grouped as follows[6]:

(a) free loop amplitude of vibration, y_{max} [10-13];
(b) angle through which the conductor is bent at the clamp by vibration, β [14-16];
(c) bending amplitude (amplitude of conductor relative to clamp, measured a short distance from the clamp), y_b, [17-19];
(d) dynamic strain in an outer-layer wire in the vicinity of the clamp[20,21].

From the above parameters, the bending amplitude (c) is the most widely used parameter[6] for measurement of vibration of operating lines, partly because of its convenience for obtaining reliable measurements in the field. However, all the above approaches suffer from the major drawback of assuming that there is some idealised strain or stress that can be calculated from vibration amplitude, and that correlates well enough with conductor fatigue life to permit its use in establishing a single endurance limit for a range of conductor sizes. The use of such an idealised stress, however, lacks a fundamental analytical basis and does suffer from certain significant shortcomings, as is discussed in the next section.

Critical examination of the previous approaches

Fig 1, shows bending fatigue performance of socketed steel cables (spiral strands and ropes) as presented by Tilly[9]: the fatigue life to fifth outer wire fracture is plotted against the range of angular deflection, $\Delta\theta$, where a very wide degree of scatter is found for cables with different levels of mean axial load and construction. In view of the rather large degree of scatter, it is not even possible to realistically define the general trend of the test data, and there appears to be a very weak correlation between the range of angular deflection, $\Delta\theta$, and free-bending fatigue life.

Hobbs & Smith[7] reported an interesting series of large-scale free-bending tests on 39 mm diameter axially preloaded spiral strands: two tests were performed with a mean axial load, $T/T_{ult.}$ = 17 %, and four data points

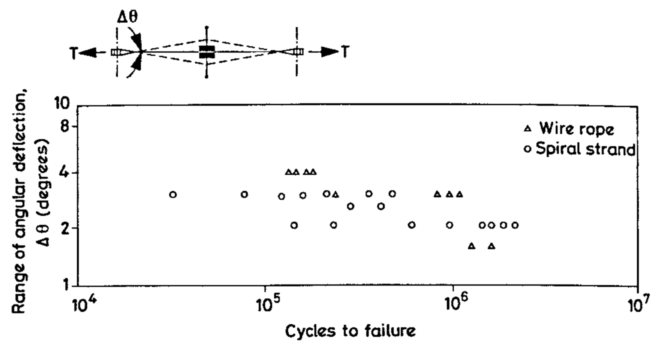

Fig 1. Bending fatigue performance of socketed spiral strands and wire ropes plotted against the range of angular deflection (after Tilly9)

were reported for a mean axial tension, $T/T_{ult.}$ = 34 %, where $T_{ult.}$ = ultimate breaking load. Based on such limited data, Hobbs & Smith[7] attempted to correlate the calculated moment at the clamped end of the 39 mm cable, M_o, with the free-bending fatigue life to first wire fracture, where it was assumed that, for their boundary conditions and mode of loading:

$$\frac{M_o}{(T_{ult.}EI_\delta)^{0.5}} = 1.1 \tan\theta' (K_\delta)^{0.5} \quad \ldots (1)$$

where

EI_δ is the assumed constant cable bending stiffness

$K_\delta = T/T_{ult}$.

θ' is the nominal angular amplitude due to cable flexure at the fixed socket

Hobbs & Smith[7] were then able to make reasonable predictions for other values of T and θ' for the *same* strand, and rather more tentatively for other cables of a similar makeup with similar terminations for which no fatigue data were then available in the public domain. Further free-bending fatigue test data on 40 and 41 mm diameter spiral strands and a 40 mm diameter multistrand rope were later reported by Strzemiecki & Hobbs[22]: these tests were carried out under conditions nominally identical with the earlier tests on the 39 mm spiral strand, and the main difference between the two series of tests was the cable construction details (such as lay angles and wire diameters in various layers) while keeping the outer diameters nominally constant. Yet again, Strzemiecki & Hobbs[22] found the initial outer layer wire fractures to invariably occur at the neutral axis (in plane-section bending terms). Fig 2 shows the plots of the non-dimensionalised moment at the clamped end, $M_o/(T_{ult.}EI_\delta)^{0.5}$, against free-bending fatigue life to first wire fracture for the 40 and 41 mm diameter spiral strands which should be compared with the originally proposed plot (based on the test data on 39 mm diameter cable) of Hobbs & Smith[7]: there appears to be a weak correlation between M_o and free-bending fatigue life where the data points for different strand constructions are not found to follow a single curve.

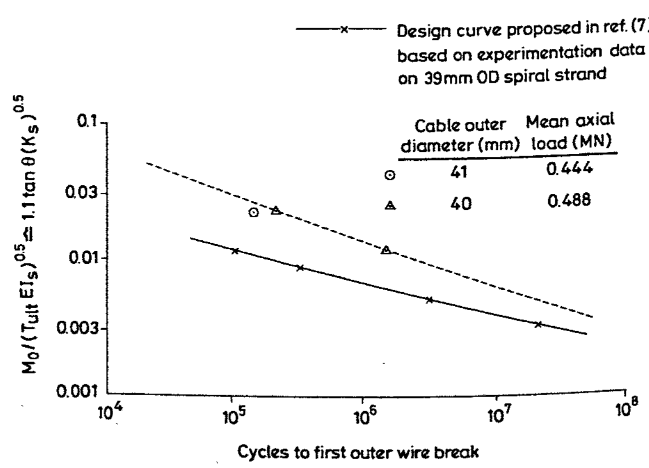

Fig 2. Plot of one-dimensionalised moment at the clamped end against free-bending fatigue life for a number of spiral strand (and one multistrand rope) constructions (after refs 5, 7, 22)

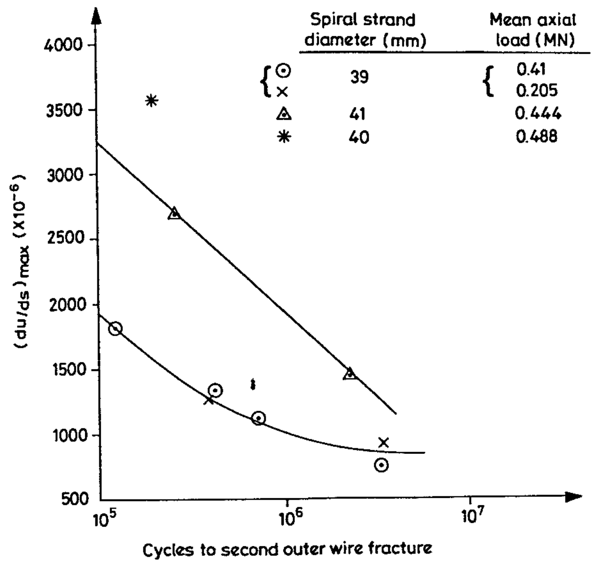

Fig 3. Plot of the maximum (extreme fibre) bending strain against free-bending fatigue life to second outer wire fracture for a number of spiral strand constructions

Finally, Fig 3 presents plots of the maximum (extreme fibre) bending strain, $[du/ds]_{max}$, against fatigue life to second outer wire fracture, for the three (39, 40, 41 mm diameter) axially preloaded spiral strands tested by Hobbs and his associates[5,7,22] and also the present author. The calculated values of $[du/ds]_{max}$ are based on a recent theoretical model developed by Raoof[23] whose predictions have been supported by some carefully conducted and large-scale free-bending tests on the 39 and 40 mm spiral strands[24,25] under conditions nominally identical with those in refs 5, 7, and 22. The parameter $[du/ds]_{max}$ relates only to the wire axial strain due to bending of the cable which, as shown by Raoof & Huang[26], is (at the fixed end) significantly larger than the corresponding strains due to bending of the wires about their own neutral axis which may safely be ignored. Results in Fig 3 strongly suggest that, although it is possible to draw a single curve to show variations of $[du/ds]_{max}$ with fatigue life for a *given* cable under various levels of mean axial load, very different curves of $[du/ds]_{max}$ v. fatigue life exist for various spiral strand construction details. In other words, the maximum wire strain (or stress) is found not to be the underlying controlling parameter in free-bending fatigue performance. This highlights the significant shortcoming of the widely used (traditional) design approach adopted by practising engineers: such approaches do not yield a generalised fatigue curve which applies to any type of steel strand construction.

To summarise, the interpretation of the often very expensive and time-consuming free-bending fatigue test data, even under closely controlled laboratory conditions, using simple parameters such as range of angular rotation, maximum moment at the clamp, and maximum calculated (or measured) wire stress (or strain), is, at its very best, appropriate only for a specific type of spiral strand construction. As discussed in what follows, in order to develop a generalised fatigue curve, there is a need for an approach that takes the interwire contact forces and slip between wires fully into account, with emphasis on the fretting fatigue behaviour over the individual interwire/ interlayer contact patches where wire fractures have mostly been found to occur.

Design recommendations

Background

Two cases have been treated, i.e. (i) bending well away from terminations and (ii) the more difficult problem of bending within the zone of influence of a termination. In the first case the free field is modelled as a multilayered spiral strand in which (for reasons of symmetry) a uniform radius of curvature is associated with plane-section bending.

For an axially pretensioned strand, it is postulated that each layer of multilayered helical strand may be treated as an orthotropic sheet and thus variations of cable bending moduli with imposed radius of curvature, ρ, have been determined[27]. It is shown that the strand effective bending rigidity under plane-section bending, $(EI)_{eff}$, varies from an upper (no-slip) to lower (full-slip) bound, with the difference between the two limiting values depending on the type of cable construction: the variation is, generally, of the order of 10-15 % for fully bedded-in strands[27,28] whose internal structure has fully stabilised with the passage of time under working conditions[29]. Such plane-section behaviour is of relevance to, for example, vortex shedding conditions where the maximum amplitudes of vibration are of the order of one cable diameter[30]. Under such conditions large-scale tests of Raoof[24,25] support the plane-section bending assumption. However, for sufficiently small radii of curvature, interlayer slippage has been shown to occur[24,25] with very substantial reductions in the effective bending rigidity: this aspect of the problem is discussed at some length in the theoretical studies of Raoof & Huang[27].

In case (ii) following experimental observations of Raoof[24,25] the pretensioned large diameter spiral strand is modelled as being composed of a solid core, which undergoes plane-section bending, covered by a single layer of helical wires[25,28,31] with interlayer friction taken fully into account. For an assumed constant state of curvature near the clamp, results are obtained for the outer wire axial stresses and for the associated extent of relative slippage between outer wires and the core. For a strand under free-bending, the radius of curvature is greatest at the fixed end and is reduced very rapidly as one moves away from the point of restraint.

The theoretical findings[23,28] which were later supported by experimental observations[24,25] throw some light on a rather unexpected observation by Hobbs & Ghavami[5] who found that, under restrained bending fatigue conditions at the fixed socket, initial wire breaks invariably occurred not at the 'extreme fibre' (in bending terms) but rather in wires very close to the neutral axis. Raoof[23,24] has shown that slip between various wires in the outer layer and the inner core in the very near vicinity of the clamp are greatest near the neutral axis and least at the extreme fibre position. It is deduced that these larger slips are a more important factor in the initiation of fatigue failures in axially preloaded spiral strands than the magnitude of the direct stress range in wires, which are greatest near the extreme fibre positions and least in the vicinity of the so-called neutral axis. It is, therefore, concluded that interwire, or rather interlayer, fretting is the most likely cause of wire breakages and is much more relevant to a discussion of free-bending fatigue life than the maximum wire stresses near the extreme fibres, as has traditionally been assumed.

A newly developed alternative[24,25,31] (Fig 4) appears much more promising. Here, the life to the second wire fracture is plotted against a contact stress-slip parameter, $\sigma_x U/x$, linking.

(1) the trellis contact patch spacing, x, along any individual wire in the outer layer;

(2) the computed interlayer relative displacement, U, near the neutral axis at a distance equal to the interlayer contact patch spacing along the wire from the assumed ideally fixed end; and

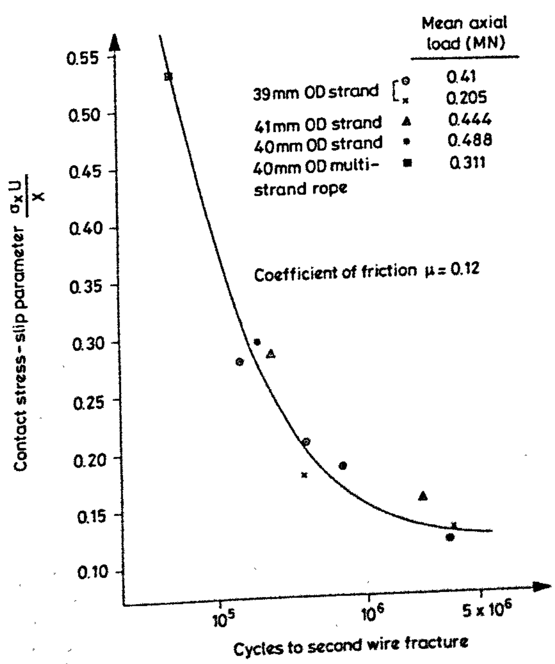

Fig 4. Plot of the newly proposed contact stress-slip parameter against free-bending fatigue life to second outer wire fracture for a number of spiral strand (and one multistrand rope) constructions

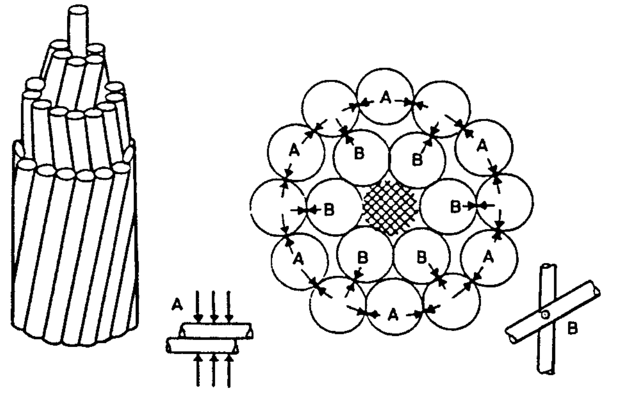

Fig 5. Pattern of interwire/interlayer contact forces in an axially preloaded spiral strand

(3) the computed maximum tensile stress, σ_x, at the trailing edge of the interlayer contact patch between wire in opposite lay, i.e. at the edge of the so-called 'trellis' contact (Fig 5).

It is encouraging that the use of this parameter makes it possible to draw a single curve of Fig 4 through data for various helical strand construction, as reported by Hobbs and his associates[5,7,22]. The coefficient of friction assumed for preparing Fig 4 was 0.12, the value found appropriate from the wide-ranging experimental work on galvanized strands[32,33]. Results in Fig 4 should prove of value for predicting cable-restrained free-bending fatigue life.

It is not the intention to repeat the often lengthy theoretical derivation here, partly because these have been reported fully elsewhere[23,25,31]. The primary purpose of the present paper is to present some simple design office routines for estimating free-bending fatigue life of realistic (large) and axially preloaded spiral strands undergoing cyclic loading.

Estimation of the radius of curvature at a fixed end

It is exceedingly rare for suspended cables to have terminations that justify use of the pinned connection in analysis, even though this is widely assumed. In fact, it is far more likely that there is local fixity at each end, the effect of which dies off rapidly (i.e. exponentially) into the cable span[6]. Moreover, it can be shown that the very localised effect of end fixity at one end of the cable is, for all practical purposes, unaffected by the nature of end conditions (such as rotational springs or complete restraint against rotation) at the far end of the member[34].

Several analyses of the shape of a vibrating stiff cable, rigidly clamped at its ends, have been published[14,35-38]. The following simplified solution, whose detailed proof is presented in Ref. 6, takes advantage of several approximations that introduce errors that are generally small enough to be neglected.

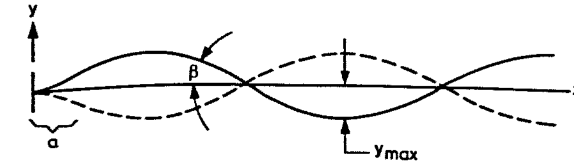

Fig 6. Standing wave vibration, with rigidly fixed supporting clamp at the left end of section 'a'

Very briefly, for a cable vibrating in standing waves as in Fig 6, and with the supporting clamp fixed, it may be assumed that the region adjacent to the clamp where the shape of the conductor departs significantly from that of a sine-shape loop is short compared with the loop length, as indicated by 'a' in Fig 6. The curvature, ρ, of the axially preloaded cable with constant mean tension, T, as it emerges from the clamp is

$$\frac{1}{\rho} = \beta\sqrt{\frac{T}{(EI)_{eff}}} \qquad \ldots (2)$$

where T is the constant axial tension and $(EI)_{eff}$ is the effective strand bending rigidity, and the angle β may be determined from the frequency, f, and amplitude of motion of the span, y_{max}, i.e.

$$\beta = \frac{2\pi f y_{max.}}{\sqrt{\dfrac{T}{m}}} \qquad \ldots (3)$$

where m is the mass/unit length. Thus the cable curvature at the clamp, ρ, becomes

$$\frac{1}{\rho} = 2\pi\sqrt{\left(\frac{m}{(EI)_{eff}} f y_{max.}\right)} \qquad \ldots (4)$$

A simple (design office type) method for estimating the effective bending stiffness, $(EI)_{eff}$, of axially preloaded spiral strands undergoing plane-section bending, which has been backed by large-scale experimental work, is reported by Raoof[19] and will not be repeated here because of space limitations.

It is also, perhaps, worth mentioning the closed form solution of Irvine[40], who used perturbation methods to show that, in the case of a taut and axially preloaded cable with constant tension, T, when the parameter $\alpha^2=[(EI)_{eff}/Tl^2]<<1$, the solution for the ith mode of vibration is

$$W(x',t) = A_i(t\sin\frac{i\pi x'}{1} + A_i(t)(i\pi)\left(\frac{(EI)_{eff}}{Tl^2}\right)^{1/2}\left\{e - \frac{x'}{\alpha l} - \cos i\pi\alpha - \left(1-\frac{x'}{l}\right)/\alpha - 1 + (1-\cos i\pi)\frac{x'}{l}\right\} \qquad \ldots (5)$$

where

- $A_i(t)$ is the amplitude of vibration
- l is the length of the cable
- x' is the coordinate along the cable with $x' = 0$ at one end and $x' = l$ at the other termination
- t is the time,
- $W(x',t)$ is the lateral deflection function with natural frequencies, ω_i

$$\omega_i = \frac{i x}{l}\left(\frac{T}{m}\right)^{1/2} \qquad \ldots (6)$$

Note that, in eqn. (5), the expression in large brackets is influenced only in small regions near each end – the flexural boundary layer: these are of length $\alpha l = ((EI)_{eff}/T)^{1/2}$, approximately. At ends $x' = 0$ and/or $x' = l$, a simple manipulation of eqn. (5) gives

$$\left[\frac{d^2W(x',t)}{dx'^2}\right] = TA_i(t)(i\pi)\left[\frac{l}{Tl^2(EI)_{eff}}\right]^{1/2} \qquad \ldots (7)$$

The maximum radius of curvature corresponding to $A_i(t) = y_{max'}$ then becomes

$$\frac{1}{\rho} = \frac{i\pi y_{max.}}{l}\left(\frac{T}{(EI)_{eff}}\right)^{1/2} \qquad \ldots (8)$$

Note that eqn. (8), could, alternatively, be obtained from eqns. (4) and (6) with $\omega = 2\pi f$. Finally, in certain applications such as in the case of tethers to tension leg platforms, the axial force in the vertical cables varies along the cable because of significant weight of these very long members in deep water applications. Closed form solutions for estimating the maximum radius of curvature at the upper and lower terminations, including the effect of rotational springs at the supports, are presented by Oran[34] who has also used a perturbation method.

Calculation of contact stress-slip parameter

In the following, much attention will be devoted to the results from an extensive series of theoretical parametric studies covering the full practical range of spiral strand (and wire) diameters and lay angles under a wide range of cable mean axial strains, $0.0005 \leq S_l' \leq 0.0045$, with this range divided into nine equally spaced values. Details of some representative strand constructions used in the parametric study are given elsewhere[41] and, for the present purposes, Table 1 gives a summary of the most important geometrical properties of most of the cables used in this theoretical exercise. Using such data, it has been found possible to propose the following simple method for estimating reasonable values of the contact stress-slip parameter for any spoiral strand construction which should prove of sufficient accuracy for design purposes without any need for lengthy calculations.

TABLE 1 – Relevant construction details for some of the multilayered spiral strands used in the theoretical parametric study

Strand diameter d(mm)	α_1 (degrees)	n_1	D_1 (mm)	α_2 (degrees)	n_2	D_2 (mm)
16	+11.91	12	3.25	−11.42	6	3.25
39	+17.74	30	3.54	−16.45	24	3.54
40	+18.07	54	2.08	−18.07	48	2.08
41	+12.45	24	4.57	−11.96	18	4.57
51	+12.83	36	4.01	−12.63	30	4.01
52	+20.93	42	3.38	−20.93	36	3.38
63	+13.99	35	5.00	−14.01	29	5.00
127	+18.01	54	6.55	−18.01	48	6.55
184	+18.01	74	7.10	−18.01	68	7.10

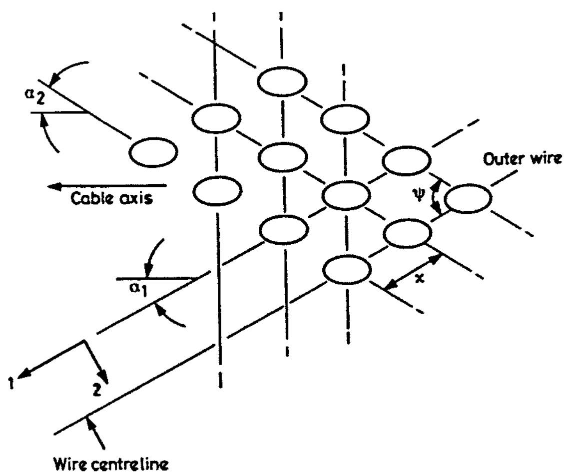

Fig 7. Pattern of interlayer trellis contact patches

Taking the simple one first, the values of trellis contact patch spacing, x, is given by [42] Fig 7:

$$x = \frac{2\pi(r_1 - r_w)\cos\alpha_2}{n_2 \sin(\alpha_1 - \alpha_2)} \quad \text{....(9)}$$

where

r_1 is the helix radius in the outer layer
r_w is the wire diameter in the outer layer
α_1 and α_2 are the lay angles in the first (outer) and second layers, respectively with right hand lay being + ve
n_2 denotes the number of wires in the second (penultimate) layer

The magnitude of the interlayer relative displacement, U, at polar angle θ_o at the ideally fixed end is given by

$$U = U'(\sin\theta - \sin\theta_o) \quad \text{....(10)}$$

where

$$U' = \frac{k^2(r_1 - r_w)}{\rho c} \quad \text{....(11)}$$

where

k is the pitch of the helix, p, divided by 2π where $p = 2\pi r_1/\tan\alpha_1$ with α_1 = lay angle in the outer layer
r_1 is the helix radius in the outer layer whose wire radius is r_w
ρ is the radius of curvature at the fixed end
$c = \sqrt{((r_1 - r_w)^2 + k^2)}$

The parameter, θ, is the polar angle of the helix measured from the point at which the helix first crosses the extreme fibre position of the bent cylinder (cable) with the parameter θ_o denoting the polar angle at which the toroidal section starts[43] (Fig 8). The magnitude of θ_o is given by:

$$\theta_o = \theta_o^{\max.} - \frac{\pi}{2} \quad \text{....(12)}$$

while

$$\theta = -\left(|\theta_o| - \frac{x}{c}\right) \quad \text{....(13)}$$

with[23]

$$\theta_o^{\max.} = -\tan^{-1}\left[\frac{1}{c}\sqrt{\left(\frac{AE_\delta}{K_{in}}\right)}\right] \quad \text{....(14)}$$

where

θ_o is always negative
A is the wire cross-section area in the outer layer
E_δ is Young's modulus for steel
K_{in} is the interlayer shear stiffness
c is as defined previously

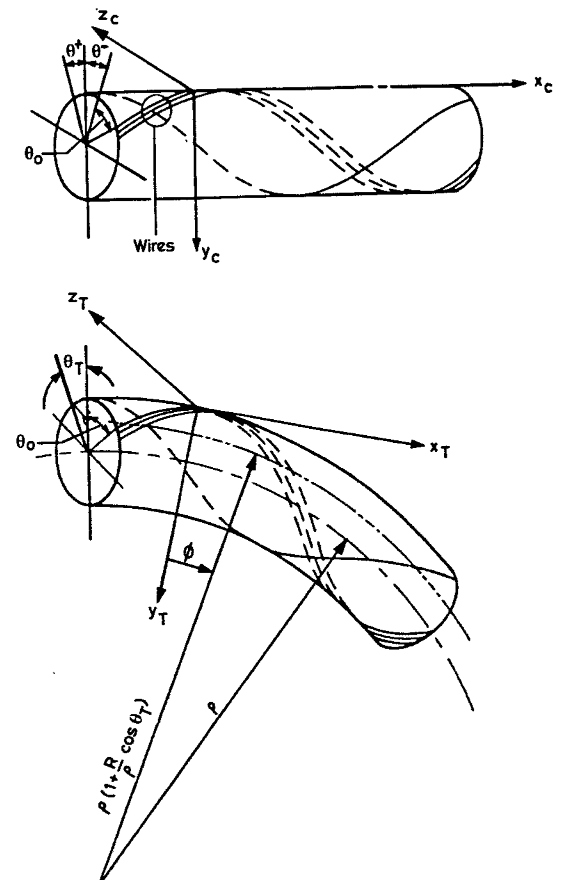

Fig 8. Geometry of a helical wire in a cable bend to a constant radius of curvature (after ref. 43)

Extensive numerical results have shown that the magnitude of K_{in} is, for all practical purposes, controlled primarily by the angle between the often counterlaid wires in the two outer and penultimate layers, $\psi = \alpha_1 - \alpha_2$, and level of cable mean axial strain, S_1', with other parameters such as wire (and cable) diameter having a relatively small effect. Based on theoretical parametric studies, the following equation gives the best fit to the theoretical predictions:

$$\frac{K_{in}}{E_\delta} = -0.00283 + 0.000109\psi + 0.0977(S_1')^{0.3179} \quad \text{....(15)}$$

$$22° < \psi < 42°, \quad 0 < S_1' < 0.0045$$

where

E is Young's modulus for steel
$\psi = \alpha_1 - \alpha_2$ (in degrees)
S_1' is the strand mean axial strain

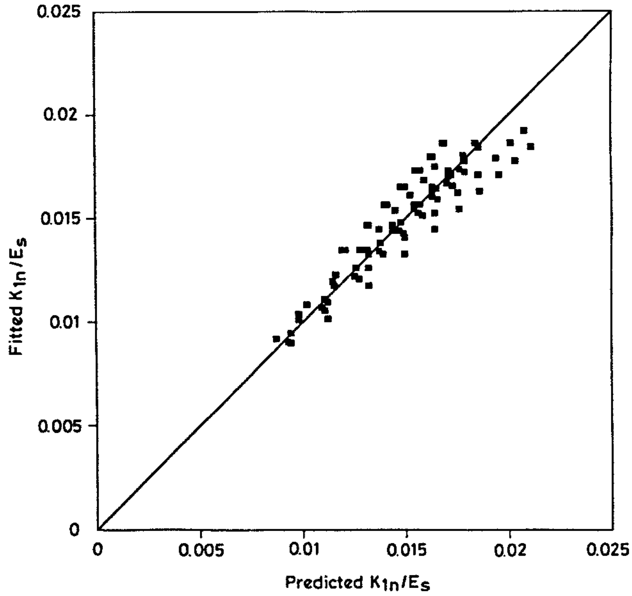

Fig 9. Comparison of the predicted (theoretical) values of $K_{in}/E\delta$ with the corresponding values obtained from eqn. (15)

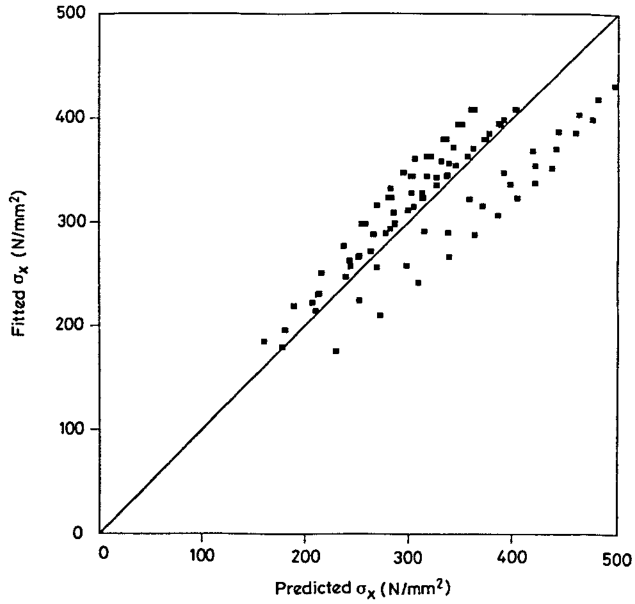

Fig 10. Comparison of the predicted (theoretical) values of σ_x with the corresponding values obtained from eqn. (16)

The standard deviation in the regression analysis was $s = 0.001051$ with a correlation coefficient R = 93%. A t-test was also carried out which confirmed the statistical significance of the association between K_{in}/E_δ and the two parameters ψ and S_1'. The parametric study led to a total number of 95 data points which were then used for the regression analysis. Fig 9 shows the plot of predicted (theoretical) values of K_{in}/E_d against the corresponding fitted values as obtained from eqn. (15): the deviations from 45° line is not very significant and particularly in view of the weak dependence of $\theta_o^{max.}$ on the exact value of K_{in}, a reasonable estimate of K_{in} is all that is needed for obtaining a very reasonable estimate of $\theta_o^{max.}$.

Finally, a total of 95 points, based on the theoretical parametric study, were used in the regression analysis, leading to the following fitted equation which defines variation of σ_x with the c able overall axial strain, S_1', and the total angle between counterlaid wires in the outer and penultimate layers, ψ,

$$\sigma_x^f = -124 + 4.41\psi + 2069\left(S_1'\right)^{0.317} \quad \ldots.(16)$$

$$22° < \psi < 42°,$$
$$0 < S_1' < 0.0045$$

where

σ_x^f is the mean of the data points relating to the value of the tensile stress at the trailing edge of the interlayer contact patch between wires in opposite lay (i.e. at the edge of the so-called "trellis" contact)
$\psi = \alpha_1 - \alpha_2$ (in degrees)
S'_1 is the strand mean axial strain.

The standard deviation in the regression analysis was s = 40.96 with a correlation coefficient R = 83.5 %. A t-test was also carried out which confirmed the statistical significance of the association between σ_x^f and the two parameters ψ and S'_1. Fig 10 shows the plot of predicted (theoretical values of σ_x against the corresponding fitted values as obtained from eqn. (16): there appears to be some scatter about the 45° line which is believed to be partly due to the neglect of other parameters such as cable (and wire) diameter. However, it must be pointed out at once that, in the theoretical formulations of σ_x, this parameter is assumed to be proportional to the coefficient of interwire friction, μ. The value of μ used in the parametric studies was assumed to be 0.12. However, as discussed elsewhere[3,29], even for a given strand, the coefficient of friction is likely to change during the working lifespan of the element because of the very significant effects of interwire abrasion and fretting plus changes in the state of commercially available blocking lubricants. In other words, the value of the assumed coefficient of friction remains rather difficult to reliably control or, indeed, predict, although it may reasonably be assumed to remain between certain bounds. In view of such practical limitations, there is little point in trying to develop more elaborate and potentially more complicated means of predicting the theoretical value of σ_x with the effect of other (less significant) parameters, such as cable (and wire) diameter, into account. The scatter in the data present in Fig 10 is certainly not more than the observed scatter in the measurements of the coefficient of friction in various steel cables.

With the above comments in mind, a more realistic and conservative method is to use an upper bound approach with, say a 95 % confidence limit for obtaining reasonable estimates of σ_x for design purposes.

An upper bound estimate of σ_x may simply be obtained from the following equation[44]:

$$\sigma_x^u = \sigma_x^f + t\sqrt{(s'^2 + s^2)} \quad \ldots.(17)$$

where, for a 95 % confidence limit to the present number of 95 samples, t=1.99. In eqn. (17), σ_x^u is the upper bound to σ_x, whose fitted mean as calculated from eqn. (16) is, σ_x^f is the standard deviation of the fit, and s' is the estimated standard deviation of fitted σ_x. For the present data, s = 40.96, and $s' \approx 7.12$ and, in view of the large population for the present data which cover a very wide range of construction details, these same values of s and s' may, in general, be used for any type of spiral strand construction detail.

Finally, with the values of parameters, σ_x, U, and x determined, the contact stress-slip parameter, $\sigma_x U/x$, may be calculated; this when used in conjunction with the plot in Fig 4, gives a reasonably conservative estimate of free-bending fatigue life to the second outer wire fracture. It must be noted that the use of experimental fatigue data to second wire fracture corresponds to approximately 5 % of wire fractures in the outer layer of spiral strands used for obtaining the plot in Fig 4. This approach, although by no means universally accepted, is believed to be more reasonable than the alternative method of presenting fatigue data to, say, first outer wire fracture: in the latter case, the accidental defects may, in certain cases, have some influence on the results, effectively somewhat masking the more relevant effect of underlying fretting fatigue mechanism. Nevertheless, it must be pointed out that, as shown by Hobbs & Smith[7], the difference between free-bending fatigue life to first or second outer wire fractures is, for all practical purposes, generally not very significant. Of more importance is the reserve of strength in a cable after the first few outer wire fractures: experimental data[5,7] suggest that there is a very substantial difference between fatigue life to first (or second) outer layer wire fracture and spiral strand total failure which may have very significant design implications, effectively providing a very desirable factor of safety against total collapse.

Numerical example

Assume a 39 mm spiral strand with geometrical details given in Table 2, having a length l = 10 m, and under a mean axial load, T = 0.30 MN, undergoing lateral vibrations in the first mode with a maximum amplitude of vibration, $y_{max.}$ = 39mm (i.e. one cable diameter). With $(EI)_{eff}^{full\text{-}slip} = 1.279 \times 10^{10}$ N/mm² (as calculated by the simple method given by Raoof[39]), eqn.

TABLE 2 – Strand make-up for the 39 mm OD strand (ultimate tensile strength = 1.23 MN)

Layer	Number of wires (*n*)	Lay direction	Wire diameter *D*(mm)	Lay angle α (degrees)
1	30	RH	3.54	17.74
2	24	LH	3.54	16.45
3	18	LH	3.54	15.93
4	12	RH	3.54	14.90
5	7	RH	3.54	15.42
King	1	—	5.05	—

(8) gives $\rho = 16.85$ m. From eqn. (9), $x = 7.14$ mm. For a strand axial Young's modulus $E_{full\text{-}slip}$ = 149 400 N/mm² (based on the *net* steel area), S'_l = 0.002098 which, from eqn. (16), gives σ_x^f = 319.7 N/mm², with the corresponding upper bound solution from eqn. (17), σ_x^u = 402.4 N/mm². Assuming, Young's modulus for steel, E_δ = 200 000 N/mm², eqn. (15) gives K_{in} = 2931 N/mm² which, when used in eqns. (14), (12) and (13), respectively, gives $\theta_o^{max} = -24.20°$, $\theta_o = 114.20°$, and $\theta = -107.11°$. Using eqn. (11), $U' = 0.0504$ which, when fed into eqn. (10) with appropriate values of θ and θ_o, gives $U = 0.00220$ mm.

Using the so-obtained values of x, σ_x^u, and U, the contact stress-slip parameter $\sigma_x^u U/x = 402.4 \times 0.00220/7.14 = 0.124$. From Fig 4, fatigue life to second wire fracture is 3.70×10^6 cycles.

For a mass/unit length, $m = 7.42$ kg/m, eqn. (6) gives $\omega = 63.14$ or $f = 10.05$ Hz. In other words, the cable will experience its second outer layer wire fracture after 102.27 h of continuous lateral vibration. Indeed, as pointed out by Hobbs & Smith[7] and also Abdel-Gaffar & Khalifa[2], this is a very alarming characteristic feature of steel cables which can undergo lateral cyclic movements for a number of reasons, depending on the type of application.

Conclusion

Practical limitations of the traditional methods for design against free-bending fatigue of axially preloaded steel spiral strands fixed at their ends against rotation have been critically addressed. It is concluded that the previous approaches invariably suffer from significant shortcomings. This situation has subsequently been improved by proposing a new (alternative) approach which takes fully into account the interwire/interlayer fretting between often counterlaid wires of a multilayered spiral strand. This is in direct contrast to the previously used (traditional) maximum bending stress approaches which invariably ignore the very important effect of interwire fretting, despite the widely reported experimental and field observations which have frequently identified interwire fretting as the primary mechanism responsible for individual wire fractures at the fixed ends.

Based on the newly proposed theoretical model, the present paper reports results from an extensive series of parametric studies on a number of realistic strand constructions with widely different cable (and wire) diameters and lay angles. Using results from this theoretical exercise, it has been found possible to propose a rather straightforward method for design against free-bending fatigue, aimed at practising engineers.

Possible practical limitations of the present simple method are critically discussed. Moreover, a numerical example is provided which should facilitate the use of the proposed formulations.

Acknowledgements

Thanks are due to Bridon Ropes personnel, Doncaster, for their patient help with information over a number of years. The author is also grateful to Mr Yu Ping Huang for executing some of the computer runs and Mrs Ada Lam for typing the manuscript.

References

1. Watson, S. C., Stafford, D.: 'Cables in trouble', *Civil Engineering*, ASCE, **58**, April 1988, p38
2. Abdel-Gaffar, Khalifa, M. A.: 'Importance of cable vibration in dynamics of cable-stayed bridges', *Journal of Engineering Mechanics*, ASCE, **117**, No. 11, November 1991, p2571
3. Hobbs, R. E., Raoof, M.: 'Hysteresis in bridge strand', *Proc. ICE*, Part 2, **77**, December 1984, p445
4. Hondalus, B.: 'Comparative vibration fatigue tests 84/19 ACSR "Chukar" versus 61-Strand 5005', *IEEE Winter Power Meeting*, New York, NY, February 1964
5. Hobbs, R. E., Ghavami, K.: The fatigue of structural wire strands, *International Journal of Fatigue*, **4**, April, p69
6. *Transmission line reference book, wind-induced conductor motion*, based on EPRI Research Project 792, Electric Power Research Institute, California, USA, 1979
7. Hobbs, R. E., Smith: 'The fatigue performance of socketed terminations to structural strands', *Proc ICE*, Part 2, **25**, March 1983, p35
8. Oplatka, G., Roth, M.: 'Wire breakages in haul ropes in the neighbourhood of couplings', *Intern. Berg-Und Seilbahn-Rundschau*, Heft 4/1974, 1974
9. Tilly, G. P.: 'Performance of bridge cables', *1st Oleg Kerensky Memorial Conference*, Session 4, London, Institution of Structural Engineers, June 1988
10. Little, J. C., MacMillan, D. G., and Majercak, J. V.: 'Vibration and fatigue life of steel strand', *AIEE Transactions*, *69*, 1950, p1473
11. Aluminium company of America – Overhead Conductor Vibration, 1961
12. Peterson, T. F., Little, J. C.: 'Conductor armor for reinforcement, splicing, and repair', *AIEE Conference Paper*, 26 August, 1949
13. Smollinger, C. W., Siter, R. B.: 'Influence of compressive forces on the fatigue performance of bethalume strand wire', *IEEE Conference Paper*, C65 237, 1965
14. Seppä, T.: 'Effect of various factors on vibration fatigue life of ACSR IBIS', *CIGRE Report 22-69 (WG04) – 04*, 1969
15. Bolser, M. O., Kanouse, E. L.: 'type HH cable in vibration and bending', *CIGRE Report 215*, 1948
16. Helms, R.: 'Zur Sicherheit der Hockspannungs-Freilietungen bei holer Mechanischer Beanspruchung', *VDI-Forschungsheft 506*, BAM, Berlin, 1964
17. Tebo, G. B.: 'Measurement and control of conductor vibration', *AIEE Transactions*, **60**, 1941, p1188
18. IEEE Committee Report: 'Standardisation of conductor vibration measurements', *IEEE Transactions Paper*, **PAS-85**, No. 1, 1966, p10
19. Josiki, Z., Kierski, A., Lewichi, K., and Lieszkowski, W.: 'New overhead transmission lines in the Polish network – service experience', *CIGRE Report*, 22-05-1976
20. Yamagata, K., Fukuda, M., and Nakayama, Y.: 'Vibration fatigue characteristics of overhead line conductors', *CIGRE Report 22-69 (WG04)*, 1970
21. Hard, A. R.: 'Studies of conductor vibration in laboratory span, outdoor test span and actual transmission lines', *CIGRE Report 404*, 1958
22. Strzemiecki, J., Hobbs, R. E.: 'Properties of wire rope under various fatigue loadings', *CESLIC Report SC6*, Department of Civil Engineering, Imperial College, September, 1988
23. Raoof, M.: 'Free bending of spiral strands', *Journal of Engineering Mechanics*, ASCE, **116**, No. 3, March 1990, p512
24. Raoof, M.: 'Free bending tests on large spiral strands', *Proc. ICE*, Part 2, **87**, December 1989, p605
25. Raoof, M.: 'Free bending fatigue of axially preloaded spiral strands', *Journal of Strain Analysis*, **27**, No. 3, 1992, pp127-136
26. Raoof, M., Huang, Y. P.: 'Wire stress calculation in helical strands undergoing bending', *Journal of Offshore Mechanics and Arctic Engineering*, ASME, **114**, August 1992, pp212-219
27. Raoof, M., Huang, Y. P.: 'Free bending characteristics of axially preloaded spiral strands', *Journal of Structures and Buildings*, ICE, **94**, November 1992, pp469-484
28. Raoof, M., Hobbs, R. E.: 'The bending of spiral strands and armoured cables close to terminations', *Journal of Energy Resources Technology*, ASME, **106**, September 1984, p349
29. Raoof, M.: 'Comparison between the performance of newly manufactured and well-used spiral strands', *Proc. ICE*, Part 2, **89**, March 1990, p103
30. Blevins, R. C.: *Flow-induced vibration*, New York, Van Nostrand Reinhold, 1977
31. Raoof, M.: 'Free bending fatigue life estimation of cables close to points of fixity', *Journal of Engineering Mechanics*, ASCE, **118**, No. 9, September 1992, pp1747-1764
32. Raoof, M., Hobbs, R. E.: 'Torsion tests on large spiral strands', *Journal of Strain Analysis*, **23**, No. 2, 1988, p97
33. Raoof, M.: 'A multi-contact problem', *Proc. 9th Int. Conf. on Experimental Mechanics*, 1990, Lyngby, Denmark, p103
34. Oran, C.: 'Asymptotic analysis of TLP tendons and risers', *Journal of Engineering Mechanics*, ASCE, **118**, No. 1, January 1992, p56
35. Morse, P. M.: *Vibration and sound*, New York, McGraw-Hill, 1948

36. Steidel, R. F.: 'Factors affecting vibratory stresses in cables near the point of support', *AIEE Transactions*, **78**, 1959, p1207
37. Scanlan, R. H., Swart, R. L.: 'Bending stiffness and strain in stranded cables', *IEEE Conference Paper C68 43-PWR*, 1968
38. Claren, R., Diana, D.: 'Dynamic strain distribution of loaded stranded cables', *IEEE Transactions Paper*, **PAS-99**, No. 41, November 1969
39. Raoof, M.: 'Design recommendations for steel cables', *Structural Engineering Review*, **4**, No. 3, 1992, pp223-233
40. Irvine, M.: 'Local bending stress in cables', *Proc. 2nd (1992) International Offshore and Polar Engineering Conf.*, San Francisco, June 1992, Vol. II, pp342-345
41. Raoof, M.: 'Cable fatigue prediction in offshore applications', *Proc. 10th Int. Conf. on Offshore Mechanics and Arctic Engineering*, ASME, Stavanger, Norway, June 1991, p403
42. Phillips, J. W., Miller, R. E., and Costello, G. A.: 'Contact stresses in straight cross-lay wire rope', *1st Annual Wire Rope Conference*, Denver, Co., March, p177
43. Lutchansky, M.: 'Axial stresses in armour wires of bent submarine cables', *Journal of Engineering for Industry*, ASME, **91**, August 1969, p687
44. Ryan, B. F., Joiner, B. L., and Ryan Jr., T. A.: *Minitab handbook*, 2nd ed., Boston, PWS-Kent Publishing Co., 1985, p233

Paper: Bellamy

Continued from page 170

The span tables for rafters, purlins, ceiling joists and binders do not assist the expert, are a danger to the untrained, and should therefore be deleted from the Building Regulations.

This leaves inclined purlins supporting sheeting, where the span tables give no guidance as to how the purlins are prevented from falling over, and joists for floors and flat roofs, both of which can be rapidly designed by hand. Again, the tables are abused by the untrained. A typical case is domestic floors where the separate joists are selected from the tables and no attempt is made to justify multiple joists carrying internal walls and trimmer beams around staircases.

Revising the span tables with extra notes setting down their limitations will not stop the errors and abuses; what is needed is to limit structural design activities to those trained to undertake them. The only way for this to be achieved is for the span tables to be deleted from the Building Regulations and replaced by a requirement that design of timber roofs is made the responsibility of a structural engineer. The trussed rafter Code already requires that the design of trussed rafters and trussed rafter roofs 'should be entrusted to chartered civil or structural engineers, or other suitably qualified persons experienced in timber engineering.' This requirement would be enforced by the building control system requiring justification of all structural designs in timber in the same way that they are required for steel and concrete.

Conclusions

The recently revised Building Regulation tables of sizes of timber floor, ceiling and roof members in single-family houses are an update of designs used for many years. The derivation of the tables makes unjustified assumptions about the strength of the joints and, as a consequence, very large numbers of roofs show movements very much greater than is permitted by timber engineering Codes. To prevent continuation of this substandard performance, it is recommended that Appendix A be deleted from Approved Document A of the Building Regulations and replaced by a requirement that the design of all timber roofs should be entrusted to chartered civil or structural engineers, or other suitably qualified persons experienced in timber engineering. This requirement would bring the design of site-cut roofs in line with the requirements for the trussed rafter industry and those for other structural materials.

References

1. Approved Document A, The Building Regulations 1991, Department of the Environment and The Welsh Office
2. BS 5268 *Structural use of timber: Part 7: Recommendations for the calculation basis for span tables; Section 7.1:* 1989 *Domestic floor joists; Section 7.2:* 1989 *Joists for flat roofs; Section 7.3:* 1989 *Ceiling joists; Section 7.4:* 1989 *Ceiling binders; Section 7.5:* 1990 *Domestic rafters; Section 7.6:* 1990 *Purlins supporting rafters; Section 7.7:* 1990 *Purlins supporting sheeting or decking*, London, British Standard Institution
3. BS 6399: *Part 3: Code of practice for imposed roof loads*, London, British Standards Institution, 1988
4. Approved Document A, The Building Regulationd 1985, Department of the Environment and The Welsh Office
5. BS 4978 *Specification for softwood grades for structural use*, London, British Standards Institution, 1988
6. BS 5268 *Structural use of timber: Part 2: Code of practice for permissible stress design, materials and workmanship*, London, British Standards Institution, 1991
7. BS 4471 *Specification for sizes of sawn and processed softwood*, London, British Standards Institution, 1987
8. CP3: *Chapter V: Part 2: Wind loads*, London, British Standards Institution, 1972
9. Concept 2000 trussed rafter design program manual, Gang-Nail Systems Ltd, 1991
10. Loose timber design program, Marlow & Co. Ltd